

T. Schmid · C. Helmbrecht · U. Panne · C. Haisch
R. Niessner

Process analysis of biofilms by photoacoustic spectroscopy

Received: 4 September 2002 / Revised: 4 November 2002 / Accepted: 4 November 2002 / Published online: 4 January 2003
© Springer-Verlag 2003

Abstract Biofilms are aggregates of microorganisms and biopolymers which occur at aqueous interfaces. Biofilms play an important role in the degradation of pollutants in natural water systems as well as in wastewater treatment plants. In this communication, the use of photoacoustic spectroscopy (PAS) as a new biofilm monitoring technique is presented. PAS combines features of optical spectroscopy and ultrasonic tomography and allows a depth-resolved analysis of optically and acoustically inhomogeneous media. For the first time, both biofilm and bulk liquid were monitored by photoacoustic sensor heads. In this way, sorption of suspended iron(III) oxide particles on the outer and inner surfaces of the biofilm could be observed on-line and in situ. Colloids can act as carriers of pollutants and influence stability and degradation efficiency of biofilms.

Keywords Photoacoustic spectroscopy · Biofilms · Particles · Colloids

Introduction

Biofilms are microbial aggregates which occur at the interfaces of aquatic systems. Biofilms consist predominantly of water and microbial cells which are embedded in a matrix of extracellular polymer substances (EPS). Microbial aggregates play an important role in the degradation of pollutants in natural waters and in wastewater treatment plants [1]. Colloids can accumulate both hydrophobic organic trace compounds and heavy metal ions onto their surfaces and act as carriers of these pollutants [2]. Therefore, the sorption of suspended particles on the outer and inner surfaces of biofilms is essential for the degradation

efficiency of bioreactors and wastewater treatment plants [3, 4]. By blocking of reactive sites and influencing the mass transport inside the film, intercepted particles can affect the degradation efficiency of biofilms. Additionally, sorbed particles can influence the stability of the biofilm and can be modified and degraded inside the biofilm [5]. For these reasons, biofilms and colloids are an important subject for environmental studies [6, 7].

The major part of noninvasive biofilm monitoring techniques is based on spectroscopic methods, such as measurements of transmittance, reflectance, or fluorescence [8, 9]. By measurement of the optical transmittance, a differential turbidity measurement device (DTM) allows the monitoring of formation and removal of both organic and inorganic deposits without any information regarding the chemical composition of the adsorbed material [10, 11]. Similar information can be obtained by measurement of the radiation which is backscattered by biofilms and other depositions using a fiber optical sensor device (FOS) [11]. By FTIR–ATR spectroscopy, absorption spectra can be measured and biofilm growth and detachment can be monitored in a more specific fashion [12, 13, 14]. The penetration depth of FTIR–ATR spectroscopy in biological samples is usually in the range of 1 to 10 μm depending on the wavelength [15]. Therefore, the signal reflects only the base layer of the biofilm. Transmission measurements in the IR range could only be performed after removal of the bulk liquid and drying of the biofilm by a rinsing gas due to the strong absorption of water in this spectral range [11].

Biofilm monitoring techniques based on optical spectroscopy do not allow depth-resolved analysis or a determination of the biofilm thickness. Ultrasonic time-domain reflectometry (TDR) has been used successfully in the monitoring of inorganic membrane fouling [16, 17]. The application of this tomographic technique to the monitoring of biofouling is hampered by the weak acoustic reflectance at the interface between biofilm and bulk liquid.

In this communication, new monitoring techniques based on photoacoustic spectroscopy (PAS) are presented

T. Schmid · C. Helmbrecht · U. Panne (✉) · C. Haisch
R. Niessner
Institute of Hydrochemistry, Technical University of Munich,
Marchioninstr. 17, 81377 Munich, Germany
e-mail: Ulrich.Panne@ch.tum.de

for on-line and in situ measurements in biofilm systems. PAS combines features of optical spectroscopy and ultrasonic tomography and allows depth-resolved analysis of both optically and acoustically inhomogeneous media. By tuning of the excitation wavelength, absorption spectra even of strongly scattering samples can be obtained, because light scattering does not generate any photoacoustic signal.

Photoacoustic spectroscopy

The photoacoustic effect is based on absorption of electromagnetic radiation inside a sample depending on the wavelength of the radiation and the chemical composition of the sample. Due to nonradiative relaxation of excited molecules, the absorbed energy is converted partially into heat. Thermal expansion of the medium leads to the generation of pressure waves which can be detected by microphones or piezoelectric transducers [18]. If short laser pulses are used for excitation, the amplitude p of the pressure wave can be described by:

$$p \propto \frac{\beta c^2}{C_p} E_0 \mu_a \quad (1)$$

where β is the thermal expansion coefficient, c is the speed of sound, C_p is the heat capacity, E_0 is the pulse energy, and μ_a is the absorption coefficient of the sample [19]. For samples consisting predominantly of water (e.g. aqueous solutions and biological matrices), the physical properties of water (with $c=1500 \text{ m s}^{-1}$) can be assumed. The temperature dependence of C_p , β , and c can be corrected by use of literature data [20]. After normalization to the laser pulse energy, optical absorption coefficients can be derived from measured pressure amplitudes. Advantages of PAS over optical transmission spectroscopy are the possibility to investigate highly concentrated, optically opaque, and scattering samples. Additionally, time-resolved recording of laser-induced pressure waves allows depth-resolved investigation of layered samples [21]. The distance z between an absorbing object inside a sample and the sample surface can be calculated simply as:

$$z = ct \quad (2)$$

with t denoting the time delay between laser pulse and arrival of the pressure wave at the surface of the sample.

PAS has been extensively used for nondestructive analysis in biological, chemical and environmental studies [19]. Former investigations of our group revealed the potential of PAS in the field of biofilm monitoring. Growth, detachment, and thickness of biofilms can be monitored on-line and in situ [22, 23, 24, 25]. The biofilm thickness measurements were verified with biofilm models with known thickness and with real biofilms using confocal laser-scanning microscopy (CLSM) as independent method [23]. The penetration depth of the photoacoustic technique in biofilms is in the range of a few millimeters and is limited predominantly by the optical penetration depth,

i.e. $1/\mu_a$. Additionally, the distribution of various major components of the biofilm system could be elucidated via wavelength-dependent measurements [26].

The interception of iron(III) oxide particles by the biofilm was observed by photoacoustic measurements [23]. As mentioned above, sorbed particles can influence the stability of the biofilm and lead therefore to a partial detachment. This was observed by depth-resolved measurements. Predominantly, the part of the biofilm with the highest particle concentration was removed from the sensor surface. The particles could not reach the base biofilm. Therefore, detachment effects in this part of the film were relatively weak.

During the experiments described in this communication, a photoacoustic flow cell for measurements in the liquid phase [27] was used in addition to the photoacoustic biofilm sensors [22, 23, 24, 25, 26]. In this way, both bulk liquid and biofilm were monitored for the first time by photoacoustic spectroscopy.

Materials and methods

Photoacoustic biofilm sensor

The photoacoustic sensors for biofilm monitoring are based on an indirect detection scheme, i.e. excitation and detection of pressure waves are performed from the same side of the sample. The sensor principle is given in Fig. 1. A piezoelectric poly(vinylidene fluoride) (PVDF) film is coupled to a transparent prism by conductive epoxy resin. The biofilm grows directly on the surface of the prism. Short laser pulses irradiate the biofilm through the prism and laser-induced pressure waves are detected by the PVDF film.

For excitation, an optical parametric oscillator (OPO, Panther, Continuum Corp., Santa Clara, USA) pumped by a frequency-tripled Nd:YAG laser (Surelite I-10, Continuum Corp., Santa Clara, USA) was used. Measurements were performed at a wavelength of 420 nm. Earlier investigations revealed that both biofilm and iron(III) oxide particles absorb electromagnetic radiation of this particular wavelength. The laser pulses were guided via optical fibers (550 μm diameter, HCG-MO550T-10, Laser Components, Santa Rosa, USA) to two sensor heads which were integrated into a flow channel (see below). The photoacoustic signals detected by the PVDF film were pre-amplified (HCA-100 M-50k-C current amplifier, Femto-Messtechnik, Berlin, Germany) and recorded by a digital storage oscilloscope (TDS 540, Tektronix, Beaverton, USA). The whole sensor system was controlled by an in-house developed LabVIEW software (LabVIEW 5.1, National Instruments, Austin, USA).

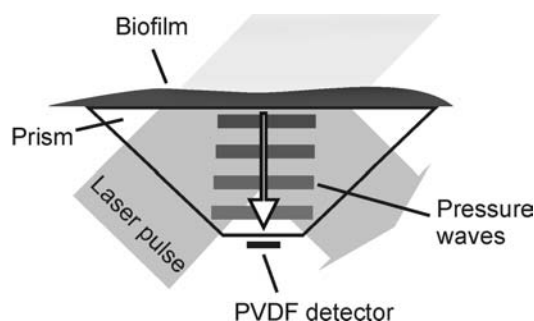


Fig. 1 Detection scheme of the photoacoustic biofilm sensors

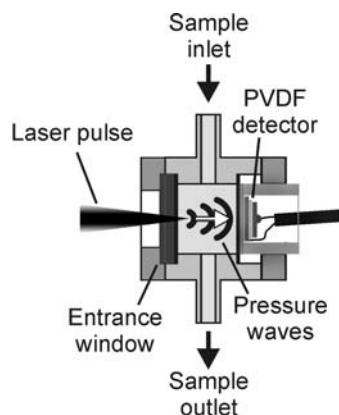


Fig. 2 Detection scheme of the photoacoustic flow cell

Photoacoustic flow cell

For monitoring of the bulk liquid phase, a photoacoustic flow cell with a direct detection scheme was used (Fig. 2). Laser pulses were focused onto the entrance window of the cell and pressure waves which were generated inside the liquid sample were detected by a piezoelectric PVDF film. A more detailed description of the flow cell can be found in Ref. [27].

For excitation, a nitrogen laser (VSL-337 ND, Starna, Pfungstadt, Germany) with an emission wavelength of 337 nm was used. Electromagnetic radiation with this particular wavelength is absorbed by iron(III) oxide particles as well as by components of the biofilm. The laser pulses were focused by a plano-convex lens ($f=30$ mm) directly onto the entrance window of the flow cell. The photoacoustic signals detected by the PVDF film were pre-amplified (HCA-100 M-50k-C current amplifier, Femto-Messtechnik, Berlin, Germany) and recorded by a digital storage oscilloscope (TDS 620, Tektronix, Beaverton, USA). Acquisition and storage of measurement data were performed by an in-house developed LabVIEW software (LabVIEW 5.1, National Instruments, Austin, USA).

Experimental setup

Two photoacoustic biofilm sensors were integrated into the base plate of a 260 mm long flow channel. The first sensor was placed 35 mm after the inlet and the second in the middle of the channel. By pumping a mixture of microorganisms and a nutrient solution through the flow channel over 24 h, biofilms were generated onto the

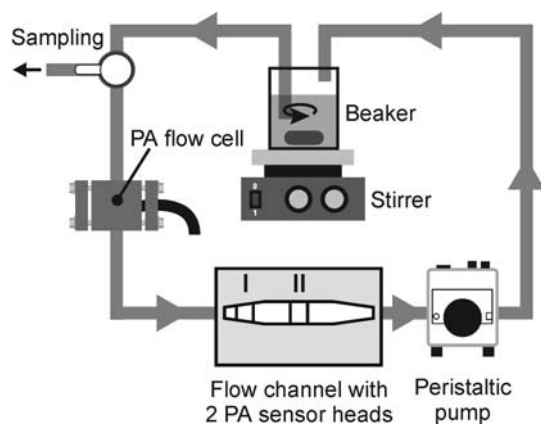


Fig. 3 Experimental setup for investigation of biofilms

surfaces of the sensor heads. A more detailed description of the experimental setup and the growth of biofilms can be found in Ref. [23].

After formation of biofilms, the channel was connected by Tygon tubing to a 1 L beaker containing 900 mL of water (Fig. 3). The water was cycled through the system by a peristaltic pump with a volume flow of 50 mL min^{-1} . The photoacoustic flow cell for monitoring of the bulk liquid phase was integrated into the tubing between beaker and inlet of the flow channel. Additionally, a three-way-valve for drawing of samples from the liquid phase was integrated into the tubing.

At the time $t=0$, the measurements with both the biofilm system and the flow cell were started. For comparison, repeated measurements of the biofilm and the bulk phase before addition of particles were performed. After 1100 s, 500 mg iron(III) oxide particles (iron(III) oxide powder, $<5 \mu\text{m}$, Aldrich) which were suspended in 100 mL of water by sonification in an ultrasonic bath were poured into the beaker. Thus, the concentration of Fe_2O_3 particles in 1 L bulk liquid was 500 mg L^{-1} at that time. During the whole experiment time of 7200 s, on-line measurements with the biofilm sensors and the photoacoustic flow cell were performed.

At intervals of 600 s, samples of the bulk phase were taken. The Fe_2O_3 concentration was determined gravimetrically after drying of 10 mL samples.

Results and discussion

Biofilm measurements

Figure 4 exhibits depth-resolved photoacoustic measurements of the biofilms at sensors I and II before and after addition of Fe_2O_3 particles. The time-resolved photoacoustic signal was converted via Eq. (2) into a depth-resolved signal. The conversion factor was the acoustic velocity of water, i.e. $c=1500 \text{ m s}^{-1}$. The origin of the depth scale corresponds to the sensor surface.

The signals at $t=139$ s and $t=186$ s reflect the optical absorption of the biofilm. Former investigations revealed that the width of photoacoustic signals of biofilms in the visible optical range is correlated with the biofilm thickness. The first minimum of the signal reflects the interface region between biofilm and bulk liquid [23]. In this case, the biofilm thickness on both sensor heads was in the range between 500 and 600 μm .

After addition of particles, a significant increase of the signal intensity due to the optical absorption of Fe_2O_3 was observed. By investigating the differences in signal shape before and after addition of Fe_2O_3 , the distribution of particles inside the biofilm can be estimated. The maximal signal increase of both sensor heads was at 50 μm and at 80 μm respectively, whereas the signal at 0 μm was relatively constant. This means that in both cases the particles could not reach the sensor surface, i.e. 0 μm .

The structure of a biofilm can be divided into a base layer consisting of a relatively dense accumulation of microorganisms and EPS matrix and a surface layer. The surface layer consists of cell clusters, channels and in general of a biofilm with lower density. Particles can obviously migrate through the channels of the surface biofilm but cannot be transported into the base layer of the film.

This fact is pointed out by Fig. 5. The signal amplitudes at 0 μm , 50 μm , and 80 μm are plotted versus the duration of the experiment. As can be seen, particle sorption

Fig. 4 Depth-resolved measurements of biofilms on sensor I (a) and sensor II (b)

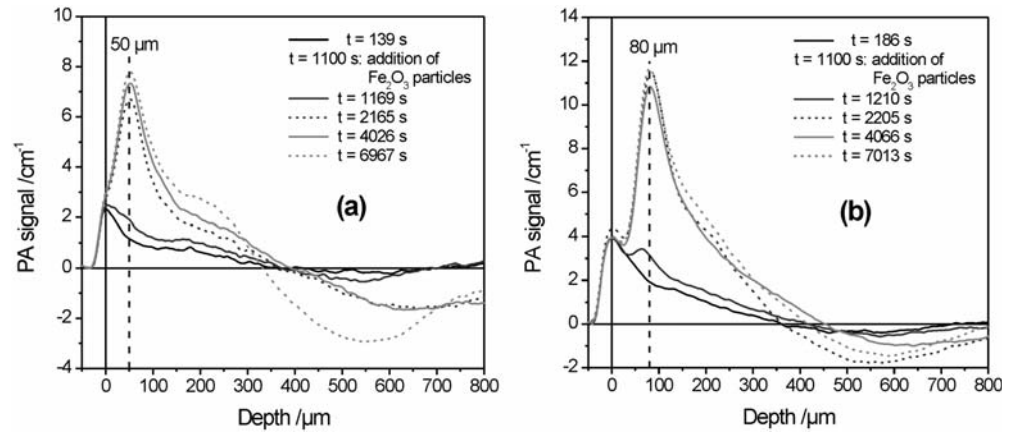
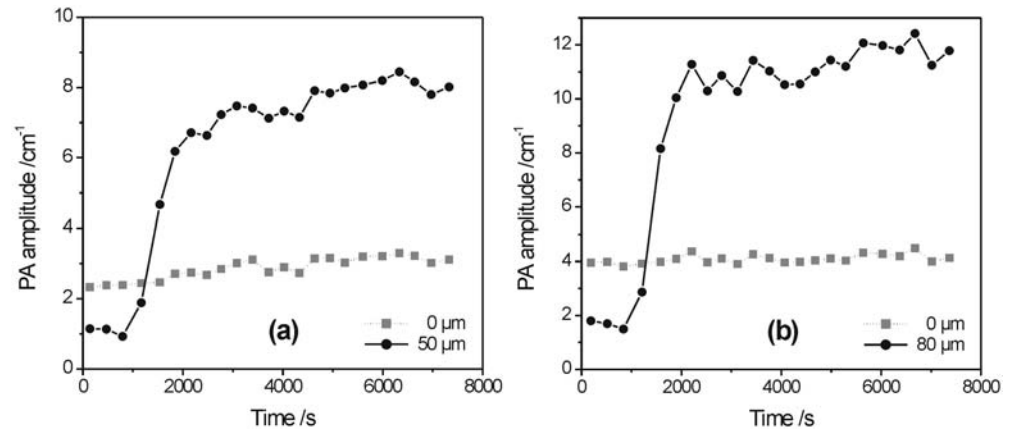


Fig. 5 Photoacoustic signals amplitudes of biofilms on sensor I (a) and sensor II (b) at different depths



leads to a strong increase of the signal at 50 μm and 80 μm respectively, whereas the effects on the signal amplitude at 0 μm are relatively weak. The maximal signal increase on sensor head II was observed at 80 μm, whereas the signal of the base biofilm remained constant. On sensor head I, the particles were transported deeper into the biofilm. Therefore, a small increase of the signal at 0 μm could be detected. Differences in penetration depth are obviously due to differences in biofilm structure. Former studies revealed that at different positions inside the flow channel, biofilms with different structures are formed. This is due to diverse flow conditions inside the channel [23].

Investigation of the bulk liquid

Figure 6 shows the behavior of photoacoustic measurements of the bulk liquid during the experiment. Before addition of Fe₂O₃ at t=1100 s, the signal reflects the optical absorption of soluble compounds and suspended biofilm flocs in the ultraviolet spectral range. After addition of particles, a fast increase of the signal could be observed. Subsequently, the signal decreased due to the removal of particles from the bulk liquid phase.

For comparison to the photoacoustic measurements, the results of the gravimetric determination of particles is exhibited. Soluble compounds and biofilm flocs led to a

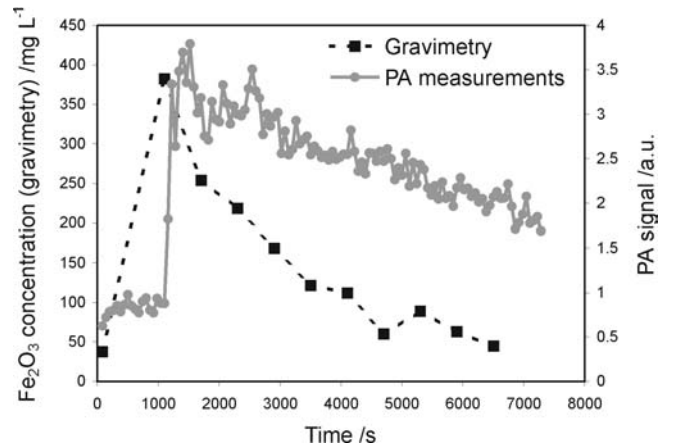


Fig. 6 Photoacoustic measurements of the bulk liquid compared to gravimetrically determined particle concentrations

blank value of 38 mg L⁻¹. After particle addition, the concentration increased to 382 mg L⁻¹. Due to sorption of particles to the biofilm, the gravimetrically determined concentration decreased and reached 45 mg L⁻¹ at t=6500 s which is very close to the blank value. Thus, gravimetry reveals that approximately the whole suspended particle mass was intercepted by the biofilm and removed from the bulk liquid phase during the experiment.

However, a significant difference between the blank value of the photoacoustic measurements and the corresponding measurement value at the end of the experiment was observed. The main problem in photoacoustic measurements of the bulk liquid was obviously the adsorption of Fe_2O_3 particles and biofilm flocs to the entrance window of the flow cell and the coupling window of the piezoelectric detector. This can lead to additional photoacoustic signals, adverse light distribution inside the cell, and modification of the acoustic transmission from the liquid sample to the PVDF detector.

Nevertheless, a calibration of the photoacoustic flow cell using the gravimetrically determined concentrations resulted in a linear function (Fig. 7). At any time when samples of the bulk liquid were taken, the mean value of five photoacoustic measurements was plotted versus the corresponding concentration. The blank value of the photoacoustic measurement was calculated as the mean of the first 18 measurements which were performed before addition of particles and subtracted from the measurement values.

The error bars in Fig. 7 reflect the standard deviation of five repeated photoacoustic measurements or weightings. The relative standard deviation of photoacoustic measurements was in the range of 3 to 7% which is in good agreement with former investigations [23]. The standard deviation of the photoacoustic measurements is dominated by fluctuations of the laser pulse energy. Another origin of measurement errors in this case can be an inhomogeneous distribution of the particles inside the measurement cell, for example due to sorption of particles to the glass windows as discussed before. Furthermore, laser pulses with a wavelength of 337 nm are absorbed by iron(III) oxide particles and by organic components of the biofilm as well. Therefore, detachment of biofilm flocs would influence photoacoustic measurements of the bulk liquid. Since detachment processes were not observed by photoacoustic biofilm measurements, this can be excluded as an additional origin of measurement errors.

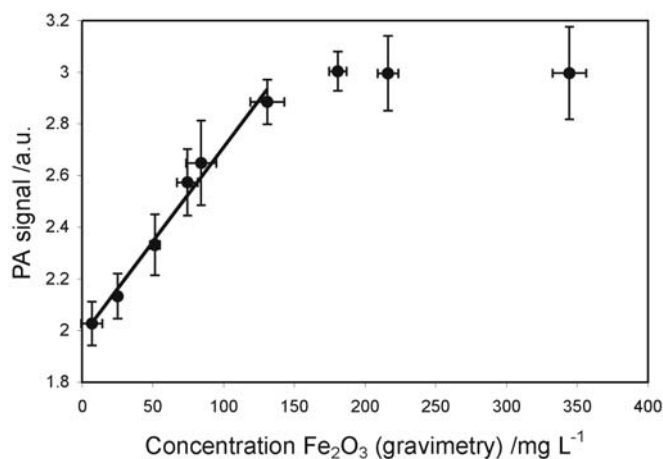


Fig. 7 Calibration of the photoacoustic flow cell. Each dot represents the mean value of five repeated photoacoustic measurements. The error bars reflect the corresponding standard deviations. The regression coefficient of the linear fit was $R^2=0.98$

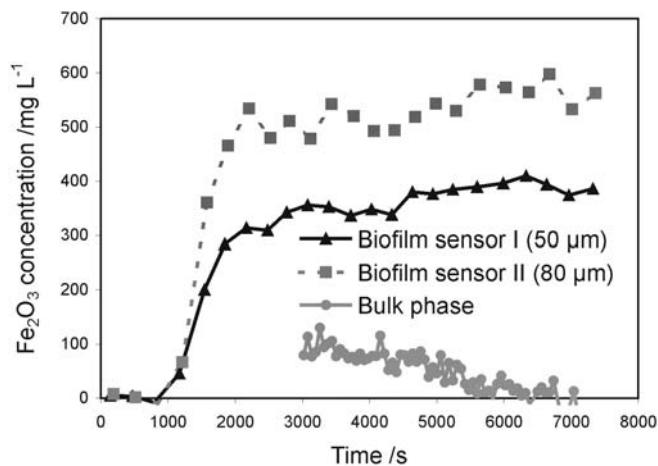


Fig. 8 Photoacoustic monitoring of both biofilm and bulk liquid phase

The calibration was linear for photoacoustic signals up to 2.9 a.u. corresponding to a concentration of approximately 130 mg L^{-1} . Obviously, saturation effects restricted the dynamic range of photoacoustic measurements with the flow cell in this case.

Photoacoustic monitoring of biofilm and bulk liquid

In order to estimate the particle concentration inside the biofilm, the photoacoustic amplitudes of the biofilm (Fig. 5) were converted into the corresponding concentrations using a calibration function that was determined within former studies [23]. The blank value was calculated as the mean of the first three measurements and subtracted from the measurement values.

In Fig. 8, the calculated concentrations are plotted versus the experiment time. Differences in biofilm structure led not only to diverse penetration depths on sensors I and II, even the particle concentrations differ from each other.

The restricted dynamic range of the flow cell measurements allowed the determination of particle concentration in the bulk liquid only for concentrations lower than 130 mg L^{-1} . This concentration was reached at $t=3020 \text{ s}$. From this moment, the decrease in particle concentration could be observed by photoacoustic measurements. The rate of removal of particles from the liquid phase is very similar to the rate of the increase of the biofilm signals. As mentioned above, approximately the whole particle mass was removed from the liquid phase during the experiment.

Conclusions

Photoacoustic spectroscopy allows depth-resolved in situ monitoring of biofilms. The technique is based on absorption of laser pulses and subsequent detection of laser induced pressure waves. The optical absorption of biofilms

can be measured in the visible and near infrared range of the electromagnetic spectrum with a penetration depth of a few millimeters which is approximately three orders of magnitude higher than the corresponding value of FTIR-ATR spectroscopy. In contrast to optical transmission measurements, photoacoustic signals are not generated by light scattering. Therefore, real absorption spectra can be obtained even in strongly scattering media such as biofilms. Another advantage over other spectroscopic biofilm monitoring techniques is the possibility to perform depth-resolved measurements by a time-resolved recording of the laser induced pressure waves with a depth resolution of approximately 10 μm in biofilms and other biological samples [23].

As well as other spectroscopic monitoring techniques, PAS is limited to biofilms growing on transparent substrata. Nevertheless, PAS allows the investigation of the influence of soluble and colloidal substances on structure and stability of biofilms and the determination of the efficiency of anti-fouling strategies under laboratory conditions [25]. Additionally, the glass surface of the sensor heads can be treated for example with aminoalkylsilanes in order to modify the physicochemical properties of the substratum [23]. For an application in real systems, the photoacoustic sensor heads could be integrated in the outer wall of bioreactors or tubes. The surface properties of tubes or support materials in fixed-bed reactors differ obviously from the properties of the glass surface of the sensor heads. Nevertheless, it would be possible to use photoacoustic sensors as indicators for biofouling in real systems.

In this communication, the use of a photoacoustic flow cell [27] for additional monitoring of the bulk liquid phase was demonstrated. During the sorption of iron(III) oxide particles to the outer and inner surfaces of a biofilm the particle concentration in the biofilm and in the bulk liquid phase could be monitored by photoacoustic measurements as well. After 2 h, approximately the whole particle mass of 500 mg was intercepted by the biofilm and removed from the bulk phase.

Additionally, the potential of photoacoustic spectroscopy for the analysis of particle suspensions could be demonstrated.

Acknowledgements The authors acknowledge the financial support by Deutsche Forschungsgemeinschaft and the grant awarded to Thomas Schmid by Max-Buchner Forschungsstiftung.

References

1. Wilderer PA, Characklis WG (1989) Structure and function of biofilms. Wiley-Interscience, New York
2. Gustafsson Ö, Gschwend PM (1997) *Limnol Oceanogr* 42:519–528
3. Eisenmann H, Letsiou I, Feuchtinger A, Beisker W, Mannweiler E, Hutzler P, Arnz P (2001) *Appl Environ Microbiol* 67:4286–4292
4. Okabe S, Yasuda T, Watanabe Y (1997) *Biotechnol Bioeng* 53: 459–469
5. Larsen TA, Harremoës P (1994) *Water Res* 28:1443–1452
6. Exner A, Theisen M, Panne U, Niessner R (2000) *Fresenius J Anal Chem* 366:254–259
7. Lawler DF (1997) *Water Sci Technol* 36:15–23
8. Jacobs L, De Bruyn EE, Cloete TE (1996) *Water Sci Technol* 34:533–540
9. Kerr A, Cowling MJ, Beveridge CM, Smith MJ, Parr ACS, Head RM, Davenport J, Hodgkiess T (1998) *Environ Int* 24:331–343
10. Klahre J, Flemming HC (2000) *Water Res* 34:3657–3665
11. Flemming HC, Tamachkiarowa A, Klahre J, Schmitt J (1998) *Water Sci Technol* 38:291–298
12. Schmitt J, Nivens D, White DC, Flemming HC (1995) *Water Sci Technol* 32:149–155
13. Suci PA, Vraný JD, Mittelman MW (1998) *Biomaterials* 19: 327–339
14. Suci PA, Geesey GG, Tyler BJ (2001) *J Microbiol Methods* 46: 193–208
15. Doran EM, Yost MG, Fenske RA (2000) *Bull Environ Contam Toxicol* 64:666–672
16. Mairal AP, Greenberg AR, Krantz WB, Bond LJ (1999) *J Membrane Sci* 159:158–196
17. Mairal AP, Greenberg AR, Krantz WB (2000) *Desalination* 130:45–60
18. Rosencwaig A, Gersho A (1976) *J Appl Phys* 47:64–69
19. Tam AC (1986) *Rev Mod Phys* 58:381–431
20. Weast RC (1983) *CRC handbook of chemistry and physics*. CRC Press, Boca Raton
21. Karabutov AA, Podymova NB, Letokhov VS (1995) *J Mod Opt* 42:7–11
22. Schmid T, Kazarian L, Panne U, Niessner R (2001) *Anal Sci* 17:S574–S577
23. Schmid T, Panne U, Haisch C, Hausner M, Niessner R (2002) *Environ Sci Technol* 36:4135–4141
24. Schmid T, Panne U, Haisch C, Niessner R (2002) *Water Sci Technol*, in print
25. Schmid T, Panne U, Haisch C, Niessner R (2002) *Biofilm monitoring by photoacoustic spectroscopy*. In: O'Flaherty V, Lens P, Mahony T, Moran A, Stoodley P (Eds) *Biofilms in medicine, industry and environmental technology*. IWA Publishing, London, in print
26. Schmid T, Panne U, Haisch C, Niessner R (2002) *Rev Sci Instrum*, in print
27. Schmid T, Helmbrecht C, Haisch C, Panne U, Niessner R (2002) *Anal Bioanal Chem*, in print (this Issue)